

# The Imaginative Generative Adversarial Network: Automatic Data Augmentation for Dynamic Skeleton-Based Hand Gesture and Human Action Recognition

Junxiao Shen, John Dudley and Per Ola Kristensson  
Department of Engineering, University of Cambridge, United Kingdom

**Abstract**—Deep learning approaches deliver state-of-the-art performance in recognition of spatiotemporal human motion data. However, one of the main challenges in these recognition tasks is limited available training data. Insufficient training data results in over-fitting and data augmentation is one approach to address this challenge. Existing data augmentation strategies, such as transformations including scaling, shifting and interpolating, require hyperparameter optimization that can easily cost hundreds of GPU hours. In this paper, we present a novel automatic data augmentation model, the Imaginative Generative Adversarial Network (GAN) that approximates the distribution of the input data and samples new data from this distribution. It is automatic in that it requires no data inspection and little hyperparameter tuning and therefore it is a low-cost and low-effort approach to generate synthetic data. The proposed data augmentation strategy is fast to train and the synthetic data leads to higher recognition accuracy than using data augmented with a classical approach.

## I. INTRODUCTION

Hand gesture interaction has the potential to afford users a fluid and unencumbered method of interfacing with computer systems. As a consequence, it has attracted considerable research attention in both hand gesture recognition (HGR) and deployment of such strategies to diverse domains including smart homes, augmented reality, virtual reality, manufacturing, and smart cars. Human action recognition (HAR) is another popular research area with many real-world applications, such as surveillance event detection, video retrieval, and smart rehabilitation [29].

One of the main challenges in HGR/HAR research is that factors, such as the complexity of hand gesture structures/action structures, differences in hand size/human size, and hand postures/human postures, can influence the performance of the recognition algorithm. While deep neural networks have had remarkable success in HGR [5], [9], [20] and HAR [35], [7], [21], problems in over-fitting or a failure to learn a high-performance model may arise when training deep neural networks with insufficient training data. Several training schemes have been developed to address this problem, including meta-learning and data augmentation.

Classical data augmentation methods increase the volume of the training set by applying transformations to raw data, which may be realistic or unrealistic, such as SpecAugment [28], cutout [6] and mixup [39]. However, these methods are not always effective on all datasets. Further, the above classical data augmentation methods are limited because they are structured such that they transform existing samples into

slightly altered additional samples. Moreover, hyperparameter optimization for the augmentation policy requires a huge budget of computation using a brute force approach that can easily cost hundreds of GPU hours. In addition, there are many different ways of altering the samples. This highlights a need to find a way of generating new data efficiently. In this paper, we propose a high-efficiency sampling strategy that can directly estimate the training data distribution and generate new samples based on the estimated distribution.

Generative Adversarial Networks (GANs) has gained much popularity in modeling data distributions directly. A GAN is a powerful tool to generate unobserved data using a minimax game without supervision [14]. Inspired by the recent success of GAN-based data augmentation in speech and vision domains [10], [16], we propose a novel variant we call the *Imaginative GAN* which assists in discovering an approximation of the true distribution of input data. The novelty of this work is the following:

- 1) We propose an unsupervised learning model for data augmentation: the Imaginative GAN, which does not require labelled data during training. Further, a trained Imaginative GAN can generalize to new data with unseen classes.
- 2) Since it does not require prior knowledge and inspection of input data for training, the Imaginative GAN allows an automatic and cross-domain data augmentation process with little hyperparameter tuning.

We evaluate our approach on two public datasets (the SHREC'17 Track dataset and the MSR Action3D dataset) using two recognition models: an LSTM model and a CNN model modified from prior work [27], [19]. We compare performance resulting from using augmented data from the Imaginative GAN (GAD) with classically augmented data (CAD). The classical approach adds realistic transformations to the data, including scaling, shifting, interpolating, and adding Gaussian noise. This approach is described in detail in Section III. As a reference, we also evaluate the effects of using the denoised and padded raw data without any augmentation, a condition we refer to as clean data (CD). We evaluate performance using two main criteria. First, the time required to find the optimized strategy for recognition accuracy in the classical approach using grid search, or the time required for the Imaginative GAN to converge. Second, the validation accuracy on each type of data.

Dataset	Model	Augmentation	Accuracy	Improvement	Standard Error	Time (hrs)	Contribution
SHREC'17 Track	LSTM	CD	72.0%	.	$\pm 0.94\%$	.	15 times faster, Accuracy increased by 3.5%
		CAD	76.6%	4.6%	$\pm 2.04\%$	75.2	
		GAD	80.1%	8.1%	$\pm 0.64\%$	5	
	CNN	CD	4.30%	.	$\pm 0.00\%$	.	5 times faster, Accuracy increased by 1.8%
		CAD	78.0%	73.7%	$\pm 0.77\%$	25.2	
		GAD	79.8%	75.5%	$\pm 0.57\%$	5	
MSR Action3D	LSTM	CD	18.4%	.	$\pm 10.64\%$	.	5 times faster, Accuracy increased by 8.8%
		CAD	58.5%	40.1%	$\pm 6.54\%$	11.2	
		GAD	67.3%	48.9%	$\pm 0.85\%$	2.1	
	CNN	CD	4.73%	.	$\pm 0.42\%$	.	2 times faster, Accuracy increased by 54.04%
		CAD	5.76%	1.03%	$\pm 1.12\%$	4.1	
		GAD	59.8%	55.07%	$\pm 2.62\%$	2.1	

TABLE I: The **Augmentation** column describes three different types of data: clean data (CD), which is denoised and padded raw data; classical augmented data (CAD), which is data augmented using a classical approach; and GAN-augmented data (GAD), which is data generated from the Imaginative GAN. The data is used to train two different models, the first is LSTM-based and the second is CNN-based. The data is from two public datasets, the SHREC'17 Track dataset and the MSR Action3D dataset. **Accuracy** is the mean validation accuracy of the trained model performed on CD, CAD, or GAD dataset. **Improvement** is the absolute improvement in accuracy resulting from the augmented data (either CAD or GAD) compared to the clean data (CD). **Standard Error** is the standard deviation of validation accuracy divided by the square root of the number of seeds (we use four random seeds). **Time** is the time taken for the hyperparameter optimization of the classical approach, or the time taken for the Imaginative GAN to converge. **Contribution** is the improvement brought by GAD for both accuracy and time compared to CAD. The data augmented by the Imaginative GAN provides higher accuracy and is more time-efficient. The results from the CNN-based recognition model suggest that the model falls into a local minimum for CD from the SHREC'17 Track dataset and for CD and CAD from the MSR Action3D dataset. In contrast, the model trained from GAD did not fail to learn to recognize, and this suggests that GAD provides a strong regularization effect to the CNN model, such that the CNN model can escape the local minimum.

In summary, we will demonstrate that the Imaginative GAN gives rise to the following four key properties:

- 1) **Higher accuracy:** As shown in Table I, the recognition models trained on GAN-augmented data (GAD) achieve the best validation accuracy for both the SHREC'17 Track dataset and the MSR Action3D dataset.
- 2) **Increased stability:** Performance is more stable on models trained on GAD compared to models trained on CD and CAD, which is observed in the smaller standard error (see Table I).
- 3) **Temporal efficiency:** Table I shows that the time taken for the classical approach to find the best combination of hyperparameters is long and varies depending on the choice of recognition model. If the model is large and difficult to converge, the time required is increased. In contrast, the Imaginative GAN is fast to train and the augmentation strategy is decoupled from the recognition model. To reduce time in the classical approach, it is possible to use a coarser grid search. However, as a result, the validation accuracy may then decrease due to suboptimal hyperparameters. Therefore, in the classical approach there is a time-accuracy trade-off.
- 4) **Generalization to new classes:** The Imaginative GAN is effective in generalizing to data with unseen classes. In other words, as long as the data to train the Imaginative GAN is in the same domain as the data with new classes, the trained model is able to generate realistic samples of the new data.

## II. RELATED WORK

The term *data augmentation* originated from Tanner and Wong [33], linking augmented data with observed data via a many-to-one mapping  $M: Y_{aug} \rightarrow Y_{obs}$ . There are different types of data augmentation strategies. A simple but effective approach is to add Gaussian noise, which is not particularly domain-specific yet can help prevent the model from overfitting [23]. Other techniques use various realistic transformations, such as elastic distortions, as well as distortions in scale, orientation, and position of training images [30], [3]. Color adjustment, blurring and sharpening, white balance, and other distortions have also been previously used on CIFAR-10 and ImageNet [18], [41]. Unrealistic distortions, such as cutout [6] and mixup [39], help regularize the training of the neural networks. However, these classical augmentation approaches usually require prior knowledge of the data and inspection of the data in addition to time-consuming hyperparameter optimization.

An alternative strategy is to augment the training set by modeling the data distribution directly using generative models, such as Bayesian approaches or GANs [34]. GANs can learn generative models via adversarial training to produce samples from the approximated real data distribution. Different variants of GANs have been proposed to generate realistic natural images [38], [32], [11]. In speech processing, GANs have been applied to speech synthesis [17], acoustic scene classification [26], and speech recognition [16]. GANs have also been used to generate synthetic path data to improve the performance of a continuous path keyboard [25]. To our knowledge, there is no prior work investigating using

GANs to synthesize skeleton data for data augmentation.

### III. GENERATING SYNTHETIC HUMAN MOTION DATA

In this paper, we compare two augmentation strategies. The first is a classical data augmentation strategy, which uses different sequential and stochastic transformations. The transformations are sometimes arbitrary and arise from manual inspection of the data. Usually, these strategies cannot be transferred across different data domains. The second strategy is the Imaginative GAN, which approximates the real data distribution and then samples from this approximated distribution.

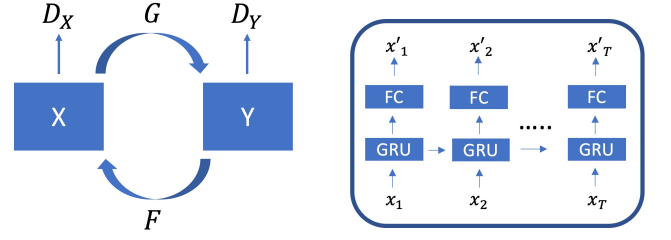
#### A. Classical Data Augmentation

From the inspection of the skeleton data, the data differs in size, postures, the speed of performing the actions/gestures and similar features. Thus such variations can be applied as transformations. We modified the data augmentation approach from Núñez et al. [27] to make the transformation more realistic. The major difference is that we sample the factors from a Gaussian distribution instead of a Uniform distribution. This is because our preliminary experiments revealed that a Gaussian distribution leads to better validation recognition accuracy with lower standard error than a Uniform distribution. Acknowledging that there are hundreds of specifications a researcher may choose to use, we have chosen the following specifications to simulate the process of how a researcher would approach the data augmentation problem using a classical approach, balancing subjective realism in transformations and a desire for high objective performance:

- 1) **Scale:** A scale factor, sampled from  $\mathcal{N}(1, \sigma_{\text{scale}}^2)$ , is applied to each data point globally, where  $\sigma_{\text{scale}}$  is a hyperparameter.
- 2) **Shift:** A global displacement  $(d_x, d_y, d_z)$ , sampled from  $\mathcal{N}(0, \sigma_{\text{shift}}^2)$ , is applied to all the data points, where  $\sigma_{\text{shift}}$  is a hyperparameter.
- 3) **Time Interpolation:** Cubic interpolation is used to interpolate the skeleton sequence. The interpolated positions are sampled from a Uniform distribution over the length of the sequence.
- 4) **Noise:** A number of joints are randomly selected and then Gaussian noise sampled from  $\mathcal{N}(0, \sigma_{\text{noise}}^2)$  is applied to the positions, where  $\sigma_{\text{noise}}$  is a hyperparameter. The number of joints selected is randomly generated between 1 to 8 for the SHREC'17 Track dataset and 1 to 4 for the MSR Action3D dataset. The number here is chosen by preliminary experiments to decrease the total number of hyperparameters. The noise added to each selected joint is different. However, the noise is the same at every timestep along the entire sequence.

#### B. Imaginative GAN

A GAN can be characterized as training a pair of networks competing against each other—it is a minimax game [14]. In a GAN, a *generator* attempts to generate as real samples as possible while a *discriminator* attempts to distinguish



(a) The Imaginative GAN is trained using a CycleGAN structure with a cycle consistency loss. The latent attributes are transferred within the input datasets  $X$  and  $Y$ .  $G$  and  $F$  are the two generators,  $D_X$  and  $D_Y$  are the two discriminators.

(b) The generator in the Imaginative GAN has one GRU layer and one fully connected layer. It has a teacher forcing mechanism so the input is a ground truth sample and the output is an altered sample.  $T$  is the length of the sample.

Fig. 1: The overall structure of the Imaginative GAN and its generator.

between the generated and real samples. Conventional GAN structures require noise as input. Training a conventional GAN is challenging because not only do the model parameters oscillate, destabilize, and sometimes never converge, but in addition the generator may collapse and produce a limited variety of samples. A large amount of data and time-consuming hyperparameter selections are required to train effective GAN models. To tackle the above challenges, we introduce teacher forcing in the generator, which uses ground truth data instead of noise as input in the conventional GANs, and thus the Imaginative GAN can more easily converge and in addition consumes less data. We also utilized the CycleGAN structure in transferring the latent attributes within the dataset, unlike the original work for unpaired image translation [40], which transfers styles between two different datasets.

1) *Networks:* The Imaginative GAN has a similar structure to CycleGAN, as shown in Figure 1a. It has two GAN structures: each GAN has one generator and one discriminator. The generator is shown in Figure 1b. The generator has a Gated Recurrent Unit (GRU) layer and a fully connected layer. No activation function is used in the fully connected layer. A GRU makes each recurrent unit adaptively capture dependencies of different time scales [2]. Unlike an LSTM unit, a GRU does not have separate memory cells. The generator has a teacher forcing mechanism that uses the ground truth data as input for every GRU cell. Teacher forcing is often used in the training of sequence to sequence models, such as machine translation models. To our knowledge, this is the first time that a teacher forcing mechanism is used in a GAN. The use of teacher forcing enables the model to easily converge and become fast to train. The input sequence to the generator is  $[x_1, x_2, \dots, x_T]$  where  $T$  is the length of the sequence and the output sequence of the generator is  $[x'_1, x'_2, \dots, x'_T]$ . The discriminator has one fully connected layer attached to a network identical to the generator to output a scalar for discrimination.

2) *Formulation:* The goal of the Imaginative GAN is to learn the latent attributes, such as behavioral attributes

(speed of performing the actions/gestures etc.,) and physical attributes (human/hand sizes etc.,). Thereafter, these learned latent attributes are applied to other data. That is, in mathematical terms, we have two generators to learn two mapping functions,  $G : X \rightarrow Y$  and  $F : Y \rightarrow X$ , between two domains,  $X$  and  $Y$ , given samples  $\{x_i\}_{i=1}^N$  where  $x_i \in X$  and  $\{y_j\}_{j=1}^N$  where  $y_j \in Y$ . Each domain has certain groups of behaviors and physical attributes. The model also has two discriminators  $D_X$  and  $D_Y$  to discriminate between the generated sample  $F(y)$  or  $G(x)$  and the real data  $x$  or  $y$ . The generator  $G$  tries to generate synthetic data  $G(x)$  that has similar attributes from domain  $Y$  with objective:

$$\mathcal{L}_{gen}(G, D_Y, X) = \mathbb{E}_{x \sim p_{data}(x)} [\log D_Y(G(x))] \quad (1)$$

The discriminator  $D_Y$  tries to distinguish  $G(x)$  from real data  $y$  with objective:

$$\begin{aligned} \mathcal{L}(G, D_Y, X, Y) = & \mathbb{E}_{y \sim p_{data}(y)} [\log D_Y(y)] \\ & + \mathbb{E}_{x \sim p_{data}(x)} [\log(1 - D_Y(G(x)))] \end{aligned} \quad (2)$$

Cycle consistency loss is used to encourage  $F(G(x)) \approx x$  and  $G(F(y)) \approx y$  [40]:

$$\begin{aligned} \mathcal{L}_{cyc}(G, F) = & \mathbb{E}_{y \sim p_{data}(y)} [\|G(F(y)) - y\|_1] \\ & + \mathbb{E}_{x \sim p_{data}(x)} [\|F(G(x)) - x\|_1] \end{aligned} \quad (3)$$

Noise is injected at each translation step and identity loss is introduced to reduce the noise:

$$\begin{aligned} \mathcal{L}_{identity}(G) = & \mathbb{E}_{y \sim p_{data}(y)} [\|G(y) - y\|_1] \\ & + \mathbb{E}_{x \sim p_{data}(x)} [\|G(x) - x\|_1] \end{aligned} \quad (4)$$

The full objective for the generator  $G$  is:

$$\begin{aligned} \mathcal{L}(G, F, D_Y) = & \mathcal{L}_{gen}(G, D_Y, X) \\ & + \lambda_1 \mathcal{L}_{cyc}(G, F) \\ & + \lambda_2 \mathcal{L}_{identity}(G) \end{aligned} \quad (5)$$

where  $\lambda_1$  and  $\lambda_2$  are the two weights of the losses. We are using an identical dataset for  $\{x_i\}_{i=1}^N$  and  $\{y_i\}_{i=1}^N$ . The generator is then effectively approximating the input data distribution through optimization by stochastic gradient descent in mini-batches.

#### IV. EXPERIMENTS

Two methods are used to evaluate and analyze the properties of the three types of data: clean data (CD), classical augmented data (CAD), and GAN augmented data (GAD). The first method is to use metrics to quantitatively evaluate the properties of the data. The second method is to use dimensionality reduction to visualize the data in their hidden representation space.

1) *Metrics for Evaluation:* Two interpretable, easy-to-compute metrics are used for parameterizing augmentation performance [13].

- 1) **Affinity:** Affinity quantifies the shift between the clean data distribution and the augmented data distribution. Affinity is calculated using the definition from Gontijo-Lopes et al. [13]: the difference between the validation

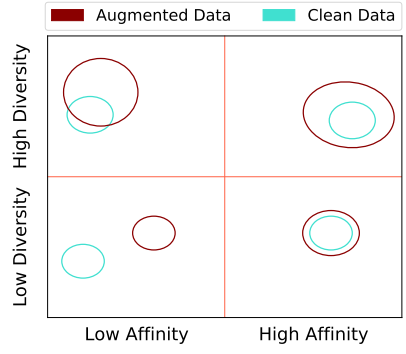


Fig. 2: Illustration of affinity and diversity. We want augmented data that has a high affinity and reasonable diversity. High affinity suggests that the augmented data is close to the clean data distribution. High diversity suggests that the augmented data is more diverse. Adapted from Gontijo-Lopes et al. [13].

accuracy of a model trained on clean data and tested on clean data and the validation accuracy of the same model tested on an augmented validation set.

- 2) **Diversity:** Diversity quantifies the complexity of the augmented data with respect to the model and optimization procedure [13]. In this paper, diversity is calculated as the difference between the validation loss and the training loss. The intuition is that the more diverse the data is, the higher the difference between the training loss and validation loss since the distance between the training data and validation data distribution will be larger. This is different from the method in Gontijo-Lopes et al. [13], where they solely use the training loss. However, only using training loss is model dependent, and may also be data dependent in certain circumstances. Therefore, to compare the two very different data augmentation policies, we use the difference between training loss and validation loss since it is more consistent and independent.

We would like the augmented data to have a high affinity and a reasonable level of diversity. The reasoning of how affinity and diversity affect the relationship between the augmented data and clean data is illustrated in Figure 2.

2) *Visualization of Latent Space:* Visualization can make data easier to understand and enhance our ability to identify patterns. Dimensionality reduction is a fundamental technique in visualization. There are two commonly used methods for visualizing high-dimensional data, one is Principal Component Analysis (PCA) and the other is t-Distributed Stochastic Neighbor Embedding (t-SNE). PCA uses the correlation between the dimensions and attempts to provide a minimum number of variables that maintain the maximum amount of information about how the original data is distributed [15]. t-SNE is a non-linear dimensionality reduction algorithm for high-dimensional data [36]. For efficiency we first used PCA and then t-SNE.

For each dataset, we use a latent representation model to

produce the latent space representation of the data. The output is then used as the input to the dimensionality reduction process. This latent representation model is a trained LSTM recognition model on the clean training data. The latent representation is fetched from the second last dense layer just before the classification layer and each representation has 512 dimensions.

#### A. Evaluation Datasets

There are several public dynamic gesture datasets [24], [4], [12]. Different human action datasets have also been introduced [22], [37], [31]. The datasets differ in the complexity of gestures or actions, the number of individuals, the gesture or action classes, and the types of sensors used for data collection. We selected datasets that provide skeleton data, and we were particularly interested in datasets of small volume. Therefore, we used the following datasets for testing:

- 1) **MSR Action3D**: The MSR Action3D dataset [22] provides 20 actions and each action is performed two or three times by ten individuals. The dataset has a total of 567 sequences. We are using the established Protocol A [27] for the training and testing split.
- 2) **SHREC'17 Track**: The SHREC'17 Track dataset [4] has 2,800 sequences which contain 14 gestures performed by 28 individuals in two ways, using a single finger and the whole hand. The dataset provides depth images and skeleton joint data. The split between training and testing is defined and well-established in the literature [4].

#### B. Recognition Model

We need a recognition model to evaluate the augmentation policies. We used two basic well-established effective neural network models, one CNN-based and one LSTM-based, as the recognition models, instead of some hypothetical highly complicated bespoke networks. Our motivation is that this approach serves to demonstrate the overall generalizability of the data augmented from the Imaginative GAN. To prevent a network bias caused by a specific type of network favoring a specific dataset, we evaluate two different neural networks (LSTM and CNN) as the recognition model.

- 1) **LSTM**: We adopted the LSTM model by Lai et al. [19]. We added a self-attention layer before the classification layer. This is to help the network find out which part of the network it should pay more attention to [1].
- 2) **CNN**: We adopted the model by Núñez et al. [27] where the structure of the network consists of a CNN attached to an MLP. It is a model they use during the pretraining stage.

Note that both the LSTM and the CNN model are not optimized using techniques such as pretraining CNN models or fine-tuning the hyperparameters (number of hidden units, number of layers, learning rate and dropout rate, etc.). Our focus is on carrying out a fair comparison of the regularization effect brought by the augmented data, not the model.

#### C. Data Preparation

The raw data is smoothed using a Savitzky–Golay filter to remove noise. This is achieved by fitting successive subsets of adjacent data points with a low degree polynomial using linear least squares. The window length is set to 7, and the order of the polynomial used to fit the data is set to 3. The smoothed data is then padded with the last row of the data to produce the clean data (CD). Subsequent data augmentations are performed on this clean data.

#### D. Training

1) **Recognition Models**: The models are trained on sparse categorical cross-entropy loss. We use Adam as the optimizer and the learning rate is set to 0.0001. The learning rate scheduler is set to be reduced on plateau, and we set the patience to 3. Early stopping is used, and we set the patience to 5. Patience is the number of epochs to wait before reducing the learning rate, or an early stop when no progress is made on the validation set. We use Sparse Categorical Accuracy to evaluate the performance of the model. The training batch size is 64.

2) **Imaginative GAN**: We use the same training scheme from the literature [40]. The training batch size is 64.  $\lambda_1$  and  $\lambda_2$  in the objective function for the generators are set to 10 and 5 respectively. The number of hidden units for the GRU cell in the generator is 512. We used a computer that has  $3 \times$  Nvidia GeForce RTX 3090 GPU,  $1 \times$  Ryzen 9 3970x CPU.

### V. RESULTS

Table I shows the overall results. We can see from the contribution column that the Imaginative GAN is not only fast to train but also leads to augmented data with higher accuracy and more stable performance when trained on the recognition models. In the remainder of this section, we focus primarily on the results obtained with the LSTM recognition model on the SHREC'17 Track dataset to illustrate the benefits afforded by the Imaginative GAN.

#### A. Generalization

For the SHREC'17 Track dataset and the LSTM network, we randomly selected four gestures and excluded them in the training of the Imaginative GAN. We then used the generators in the trained Imaginative GAN to generate synthetic data of the four gestures from the real gesture data. Figure 4 shows that the four gestures do not show any degradation in their accuracy compared to the clean data and the optimized classical augmentation data. The optimized classical augmentation strategy is discussed in V-B. This demonstrates that the model can generalize to data with new classes. We performed the same test with the CNN and MSR Action 3D dataset and also observed this generalization capability.

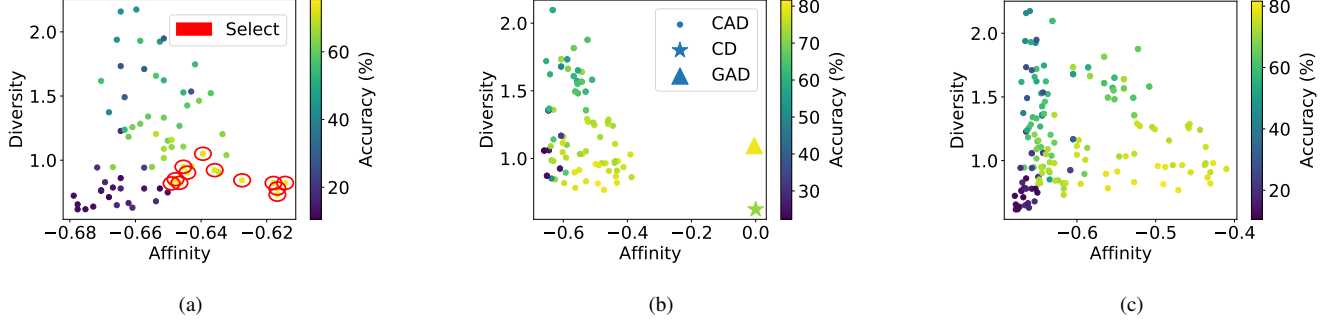


Fig. 3: Affinity measures the shift between the augmented data and the clean data distribution. Diversity measures how diverse the data is. (a) The results of the first round search (coarse grid search) for optimal hyperparameters of the classical approach. Circled data points in red are what we will select to inspect and use for a second round search. (b) The results of the second round search (fine grid search). The results from GAD and CD are also shown to compare affinity, diversity, and accuracy. (c) The combination of the results of the first and second round search are presented to show an overview of how affinity and diversity relates to accuracy. It also illustrates the representations in Figure 2. We observe that we want affinity to be as high as possible and a diversity at around 1. Results are from experiments when using LSTM as the recognition model and SHREC’17 Track as the evaluation dataset.

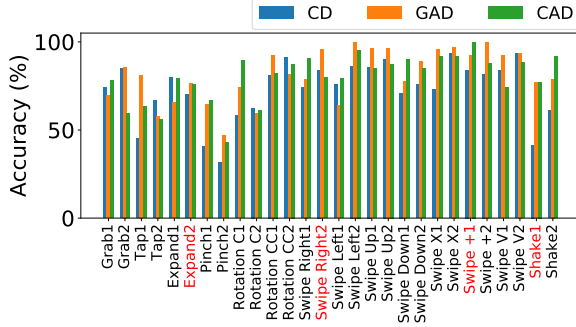


Fig. 4: Individual accuracy from the LSTM recognition model of the gestures for the three types of data: clean data (CD), GAN-augmented Data (GAD), and classical augmented data (CAD). Gesture classes in red are the new classes that are excluded from the training of the Imaginative GAN. Synthetic data of the new classes achieved comparable accuracy with the synthetic data of the classes seen in the training phase. The 1 or 2 after the gesture classes indicates the number of fingers used to perform the gesture. 1 represents one finger and 2 indicates the entire hand.

### B. Time Efficiency

This investigation also used the SHREC’17 Track dataset and the LSTM network. In the classical data augmentation approach, there are three hyperparameters to optimize:  $\sigma_{scale}$ ,  $\sigma_{shift}$  and  $\sigma_{noise}$ . There could be more hyperparameters, and this depends on how many transformations are applied to the data. Three common ways of performing hyperparameter optimization are random search, grid search, and Bayesian optimization. Here we are using grid search to optimize hyperparameters since it is a simple but effective method for exploring a regular search space. We carried

out two rounds of search. The first round is a coarse grid search. We used  $\sigma_{scale} \in [0.1, 0.15, 0.2, 0.25, 0.3]$ ,  $\sigma_{shift} \in [0.1, 0.15, 0.2, 0.25, 0.3]$  and  $\sigma_{noise} \in [0.1, 0.2, 0.3]$ .

Figure 3a shows the result from the first-round search. We observe that the combinations in the red selected circles have good accuracy. We investigated the combinations that produced these results and performed a second round of search, a fine grid search, that has  $\sigma_{scale} \in [0.1, 0.12, 0.14, 0.18, 0.2]$ ,  $\sigma_{shift} \in [0.1, 0.12, 0.14, 0.18, 0.2]$  and  $\sigma_{noise} \in [0.05, 0.1, 0.15]$ . Figure 3b shows the results from the second round search together with the validation accuracy achieved from the clean data and GAN augmented data. We found that the optimized hyperparameters achieved a validation accuracy of 76.6%, which is less than the accuracy (80.1%) achieved by the GAN-augmented data. Compared with the 5 GPU hours training time for the Imaginative GAN, the classical data augmentation approach costs around 15 times more GPU hours (75.2).

### C. Escaping Local Minimum

We now use the CNN model to evaluate the recognition performance of the data (Table I). We observe that for MSR Action3D, CNN failed to learn the features from CD and CAD, which suggests that the model is trapped in a local optima. In contrast, the GAN-augmented data helped the recognition model to escape the local minimum.

### D. Affinity and Diversity

For the SHREC’17 Track dataset and the LSTM network, in Figure 3c, we observe, as expected, that the points with high affinity and diversity around 1.0 have the highest accuracy, and data with low affinity and low diversity cannot produce a good result. We also observe that a too high diversity can decrease accuracy as the model may fail to



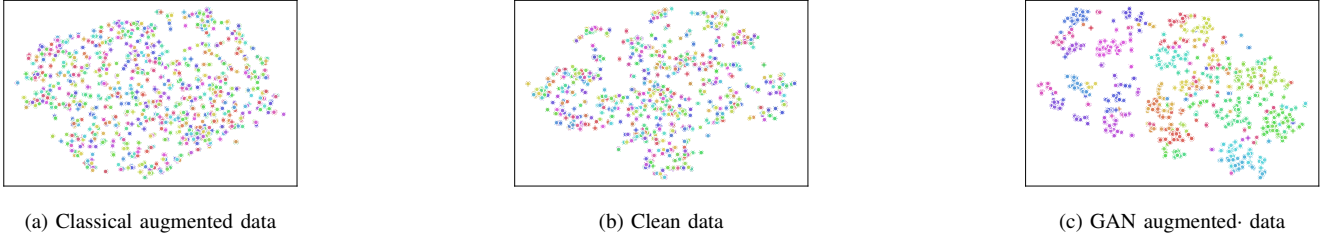


Fig. 5: Dimensionality reduction of the latent space representations of the three types of data in the SHREC’17 Track dataset. The representations are clustered into 28 different gesture classes. The classical augmented data (CAD) shows no obvious sign of clusters (a). The clean data (CD) shows clear clusters, however, some of the data points are misplaced in the clusters as the color of each cluster is not distinctive (b). The GAN-augmented data (GAD) shows clear boundaries between clusters and each cluster has a distinguishable color (c). This is what we would expect from the results in Figure 3c, as GAD exhibits good diversity and affinity, CD shows a low diversity, and CAD shows a good diversity but poor affinity. Affinity plays a more important role in clustering since the feature extraction model is trained on clean data, and a high affinity is desired to produce better results.

learn the complexity of the data. Therefore, we expect data with as high affinity as possible and diversity of around 1.0 will achieve the best recognition accuracy. This is achieved by the GAN-augmented data. The results from the CNN and the MSR Action3D dataset were found to highlight the same advantages of GAD over CD and CAD.

#### E. Visualization of Latent Space

As can be observed in Figure 5a, the classical augmented data reveals no clustering at all when visualizing the latent space due to the low affinity. In Figure 5b, the clean data reveals some clusters and the distribution is dispersed to a visible extent. The GAN-augmented data reveals very clean boundaries between the clusters (Figure 5c). Although the visualization model was trained on the clean data, it works better on the GAN-augmented data. This suggests that when t-SNE is optimized, the diversity of the GAN-augmented data helps its optimization process.

#### F. Ablation Study

We performed an ablation study on the MSR Action3D dataset to evaluate the importance of the number of hidden units of the GRU cell in the Imaginative GAN. We tested four numbers of hidden units: 64, 128, 256 and 512. They lead to a validation accuracy of 46.4%, 55.1%, 64.2% and 67.3% respectively. This result can be justified by the reasoning that more hidden units can encode more information of the input sequence. A high number of hidden units only increase the training time by within 10% which is acceptable. Therefore, 512 hidden units are used for a higher validation accuracy.

### VI. LIMITATIONS AND FUTURE WORK

A potential limitation is the requirement for some tuning of the learning rate and number of hidden units in the Imaginative GAN. However, in contrast to the huge hyperparameter space for the classical augmentation approach, tuning the two hyperparameters with limited choices is easy and fast. If a trained model exists, then generating thousands of data takes less than a second.

In theory, the Imaginative GAN is able to approximate any trajectory. Trajectory data records locations of moving objects at certain moments, and has been used widely when researching, for example, human behavior and traffic problems. We believe fruitful future work is to verify this statement by carrying out experiments on generating sequences of behaviors/movement from other domains, such as people, vehicles, animals, etc. Related to this, deep learning models in path planning for self-driving cars or robotics require an intensive amount of training data and we see applying the Imaginative GAN to such domains as promising future work.

Moreover, the Variational Autoencoder (VAE) is popular among the generative models for its powerful ability to learn the underlying data distribution using unsupervised learning [8]. VAE and GAN mainly differ in the way of training. VAE optimizes the Evidence Lower Bound (ELBO) while GAN optimizes using a minimax game. We are interested in whether a VAE can generate synthetic skeleton data, and how this data might compare with that produced by the Imaginative GAN.

### VII. CONCLUSIONS

We have proposed an automatic data augmentation tool that can ‘imagine’ realistic alterations to input data. It is the first time a teacher forcing training scheme has been used in a GAN, and the approach of using a CycleGAN structure to generate trajectory data is also novel. Moreover, CycleGAN was originally proposed to transfer latent attributes between two datasets. However, we here use it within one dataset. The data augmented using the Imaginative GAN is evaluated against data augmented using a classical approach as well as the denoised and padded raw data. Our results have demonstrated that the Imaginative GAN outperforms the classical approach in mean validation accuracy, standard error, and in the time cost to find an optimized strategy. We have also observed that the data distribution approximated by the Imaginative GAN is close to the real data distribution and exhibits a higher diversity than the real data.

In summary, the Imaginative GAN is superior to simply adding stochastic and sequential distortions to data. In the future, we foresee a library of Imaginative GANs trained on different types of data, allowing researchers to directly download pre-trained Imaginative GANs and instantly generating their own synthetic data. While the classical approach may still be a useful tool to prevent over-fitting and increase the deep learning model's performance, the Imaginative GAN can always be used as a baseline to compare against, since it takes almost zero effort and zero prior knowledge or inspection of the input data to generate synthetic data using the Imaginative GAN.

## REFERENCES

- [1] J. Cheng, L. Dong, and M. Lapata. Long short-term memory-networks for machine reading. *arXiv preprint arXiv:1601.06733*, 2016.
- [2] J. Chung, C. Gulcehre, K. Cho, and Y. Bengio. Empirical evaluation of gated recurrent neural networks on sequence modeling. *arXiv preprint arXiv:1412.3555*, 2014.
- [3] E. D. Cubuk, B. Zoph, D. Mane, V. Vasudevan, and Q. V. Le. Autoaugment: Learning augmentation policies from data. *arXiv preprint arXiv:1805.09501*, 2018.
- [4] Q. De Smedt, H. Wannous, J.-P. Vandeborre, J. Guerry, B. Le Saux, and D. Filliat. SHREC'17 Track: 3D Hand Gesture Recognition Using a Depth and Skeletal Dataset. In I. Pratikakis, F. Dupont, and M. Ovsjanikov, editors, *3DOR - 10th Eurographics Workshop on 3D Object Retrieval*, pages 1–6, Lyon, France, Apr. 2017.
- [5] G. Devineau, F. Moutarde, W. Xi, and J. Yang. Deep learning for hand gesture recognition on skeletal data. In *2018 13th IEEE International Conference on Automatic Face & Gesture Recognition (FG 2018)*, pages 106–113. IEEE, 2018.
- [6] T. DeVries and G. W. Taylor. Improved regularization of convolutional neural networks with cutout. *arXiv preprint arXiv:1708.04552*, 2017.
- [7] Z. Ding, P. Wang, P. O. Ogunbona, and W. Li. Investigation of different skeleton features for cnn-based 3d action recognition. In *2017 IEEE International Conference on Multimedia & Expo Workshops (ICMEW)*, pages 617–622. IEEE, 2017.
- [8] C. Doersch. Tutorial on variational autoencoders. *arXiv preprint arXiv:1606.05908*, 2016.
- [9] Y. Du, W. Wang, and L. Wang. Hierarchical recurrent neural network for skeleton based action recognition. In *Proceedings of the IEEE conference on computer vision and pattern recognition*, pages 1110–1118, 2015.
- [10] M. Frid-Adar, I. Diamant, E. Klang, M. Amitai, J. Goldberger, and H. Greenspan. Gan-based synthetic medical image augmentation for increased cnn performance in liver lesion classification. *Neurocomputing*, 321:321–331, 2018.
- [11] M. Frid-Adar, E. Klang, M. Amitai, J. Goldberger, and H. Greenspan. Synthetic data augmentation using gan for improved liver lesion classification. In *2018 IEEE 15th international symposium on biomedical imaging (ISBI 2018)*, pages 289–293. IEEE, 2018.
- [12] G. Garcia-Hernando, S. Yuan, S. Baek, and T.-K. Kim. First-person hand action benchmark with rgb-d videos and 3d hand pose annotations. In *Proceedings of Computer Vision and Pattern Recognition (CVPR)*, 2018.
- [13] R. Gontijo-Lopes, S. J. Smullin, E. D. Cubuk, and E. Dyer. Affinity and diversity: Quantifying mechanisms of data augmentation. *arXiv preprint arXiv:2002.08973*, 2020.
- [14] I. J. Goodfellow, J. Pouget-Abadie, M. Mirza, B. Xu, D. Warde-Farley, S. Ozair, A. Courville, and Y. Bengio. Generative adversarial networks. *arXiv preprint arXiv:1406.2661*, 2014.
- [15] H. Hotelling. Analysis of a complex of statistical variables into principal components. *Journal of educational psychology*, 24(6):417, 1933.
- [16] H. Hu, T. Tan, and Y. Qian. Generative adversarial networks based data augmentation for noise robust speech recognition. In *2018 IEEE International Conference on Acoustics, Speech and Signal Processing (ICASSP)*, pages 5044–5048. IEEE, 2018.
- [17] T. Kaneko, S. Takaki, H. Kameoka, and J. Yamagishi. Generative adversarial network-based postfilter for stft spectrograms. In *Interspeech*, pages 3389–3393, 2017.
- [18] A. Krizhevsky, I. Sutskever, and G. E. Hinton. Imagenet classification with deep convolutional neural networks. *Advances in neural information processing systems*, 25:1097–1105, 2012.
- [19] K. Lai and S. N. Yanushkevich. Cnn+ rnn depth and skeleton based dynamic hand gesture recognition. In *2018 24th International Conference on Pattern Recognition (ICPR)*, pages 3451–3456. IEEE, 2018.
- [20] G. Lefebvre, S. Berlemont, F. Mamalet, and C. Garcia. Blstm-rnn based 3d gesture classification. In *International conference on artificial neural networks*, pages 381–388. Springer, 2013.
- [21] C. Li, P. Wang, S. Wang, Y. Hou, and W. Li. Skeleton-based action recognition using lstm and cnn. In *2017 IEEE International Conference on Multimedia & Expo Workshops (ICMEW)*, pages 585–590. IEEE, 2017.
- [22] W. Li, Z. Zhang, and Z. Liu. Action recognition based on a bag of 3d points. In *2010 IEEE Computer Society Conference on Computer Vision and Pattern Recognition-Workshops*, pages 9–14. IEEE, 2010.
- [23] R. G. Lopes, D. Yin, B. Poole, J. Gilmer, and E. D. Cubuk. Improving robustness without sacrificing accuracy with patch gaussian augmentation. *arXiv preprint arXiv:1906.02611*, 2019.
- [24] G. Marin, F. Dominio, and P. Zanuttigh. Hand gesture recognition with leap motion and kinect devices. In *2014 IEEE International conference on image processing (ICIP)*, pages 1565–1569. IEEE, 2014.
- [25] A. Mehra, J. R. Bellegarda, O. Bapat, P. Lal, and X. Wang. Leveraging gans to improve continuous path keyboard input models. In *ICASSP 2020-2020 IEEE International Conference on Acoustics, Speech and Signal Processing (ICASSP)*, pages 8174–8178. IEEE, 2020.
- [26] S. Mun, S. Park, D. K. Han, and H. Ko. Generative adversarial network based acoustic scene training set augmentation and selection using svm hyper-plane. *Proc. DCASE*, pages 93–97, 2017.
- [27] J. C. Nunez, R. Cabido, J. J. Pantrigo, A. S. Montemayor, and J. F. Velez. Convolutional neural networks and long short-term memory for skeleton-based human activity and hand gesture recognition. *Pattern Recognition*, 76:80–94, 2018.
- [28] D. S. Park, W. Chan, Y. Zhang, C.-C. Chiu, B. Zoph, E. D. Cubuk, and Q. V. Le. SpecAugment: A simple data augmentation method for automatic speech recognition. *arXiv preprint arXiv:1904.08779*, 2019.
- [29] R. Poppe. A survey on vision-based human action recognition. *Image and vision computing*, 28(6):976–990, 2010.
- [30] I. Sato, H. Nishimura, and K. Yokoi. Apac: Augmented pattern classification with neural networks. *arXiv preprint arXiv:1505.03229*, 2015.
- [31] A. Shahroudy, J. Liu, T.-T. Ng, and G. Wang. Ntu rgb+ d: A large scale dataset for 3d human activity analysis. In *Proceedings of the IEEE conference on computer vision and pattern recognition*, pages 1010–1019, 2016.
- [32] Y. Taigman, A. Polyak, and L. Wolf. Unsupervised cross-domain image generation. *arXiv preprint arXiv:1611.02200*, 2016.
- [33] M. A. Tanner and W. H. Wong. The calculation of posterior distributions by data augmentation. *Journal of the American Statistical Association*, 82(398):528–540, 1987.
- [34] T. Tran, T. Pham, G. Carneiro, L. Palmer, and I. Reid. A bayesian data augmentation approach for learning deep models. *arXiv preprint arXiv:1710.10564*, 2017.
- [35] A. Ullah, J. Ahmad, K. Muhammad, M. Sajjad, and S. W. Baik. Action recognition in video sequences using deep bi-directional lstm with cnn features. *IEEE access*, 6:1155–1166, 2017.
- [36] L. Van der Maaten and G. Hinton. Visualizing data using t-sne. *Journal of machine learning research*, 9(11), 2008.
- [37] J. Wang, Z. Liu, Y. Wu, and J. Yuan. Mining actionlet ensemble for action recognition with depth cameras. In *2012 IEEE Conference on Computer Vision and Pattern Recognition*, pages 1290–1297. IEEE, 2012.
- [38] T. Xu, P. Zhang, Q. Huang, H. Zhang, Z. Gan, X. Huang, and X. He. Attngan: Fine-grained text to image generation with attentional generative adversarial networks. In *Proceedings of the IEEE conference on computer vision and pattern recognition*, pages 1316–1324, 2018.
- [39] H. Zhang, M. Cisse, Y. N. Dauphin, and D. Lopez-Paz. mixup: Beyond empirical risk minimization. *arXiv preprint arXiv:1710.09412*, 2017.
- [40] J.-Y. Zhu, T. Park, P. Isola, and A. A. Efros. Unpaired image-to-image translation using cycle-consistent adversarial networks. In *Proceedings of the IEEE international conference on computer vision*, pages 2223–2232, 2017.
- [41] B. Zoph, V. Vasudevan, J. Shlens, and Q. V. Le. Learning transferable architectures for scalable image recognition. In *Proceedings of the IEEE conference on computer vision and pattern recognition*, pages 8697–8710, 2018.